Supplementary Information for:

Study of Torque, Drag and Hydraulics of a Deviated Drilled Well using Drilling Office Software

Table S1. Details of well sections

Hole number	Hole size	Bit	Casing size	Drilling mud	Penetrated formations
1	32 inches	26 inch and 32inch hole opener	26 in	Sea water and viscous pill (PHG and Guar gam)	Fars group formations
2	23 ½ inches	23 ½ inches	18 5/8 in	Sea water and viscous pill (PHG and Guar gam)	Asmari, Jahrom and Ilam formations
3	16 inches	PDC	13 3/8 in	Polymer mud with viscous pill	Lafan, Sarvak, kazhdomi Darian, Gadvan, fahlian and Hith formations
4	12¼ inches	PDC	9 5/8 in	Polymer mud	Hith, Sormeh, Neyriz, Dashtak, Aghar shale and several feet from Kangan formation
5	8½ inches	PDC	7 in liner	Polymer mud	Kangan, Dalan and several meters from Nar formations

Table S2. Input data of torque and drag in drilling office.

	Hole size (in)			
Input data	**23 ½**	**16**	**12 ¼**	**8 ½**
Downhole torque (1000 lb. ft)	4	3.5	2	2
Tension on bit (1000 lb. ft)	4	3.5	2	2
Block weight (1000 lb. ft)	35	35	35	35
Operating mode	rotation	rotation	rotation	rotation
Mud weight (lbm/gal)	8.7	9.4	11.6	11.5
Formation stiffness	0.5	0.5	0.5	0.5
Bottom depth (ft)	607 (0.2)	3510.5 (0.2)	6151.6 (0.2)	14383.2 (0.2)
Rotation component	1225.4 (0.3)	6029 (0.3)	14379.9 (0.3)	16210.4 (0.3)
Bit depth(ft)	1225.44	6028.99	14379.91	16210.42

Table S3. Single point of torque and drag analysis.

Hole/parameter	Surface torque (1000 ft.lb)	Hook load (1000 lb)
23 ½	4.5	71.3
16	6.4	284.9
12 ¼	5.6	348.1
8 ½	5	367.3

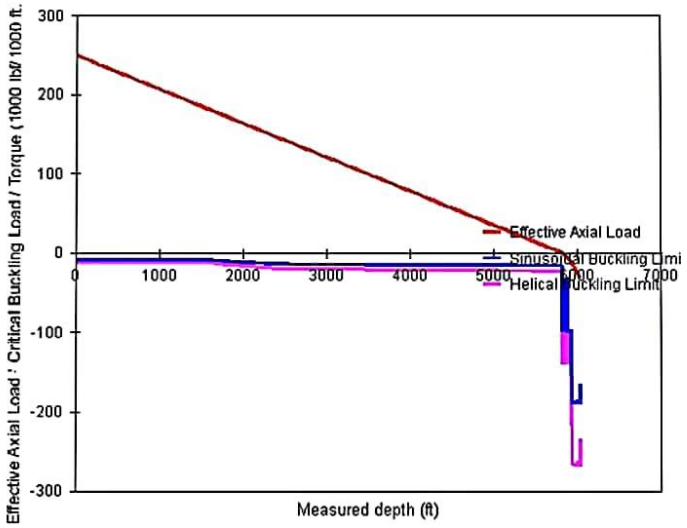

Fig. S1. Effective axial load in 16-inch hole.

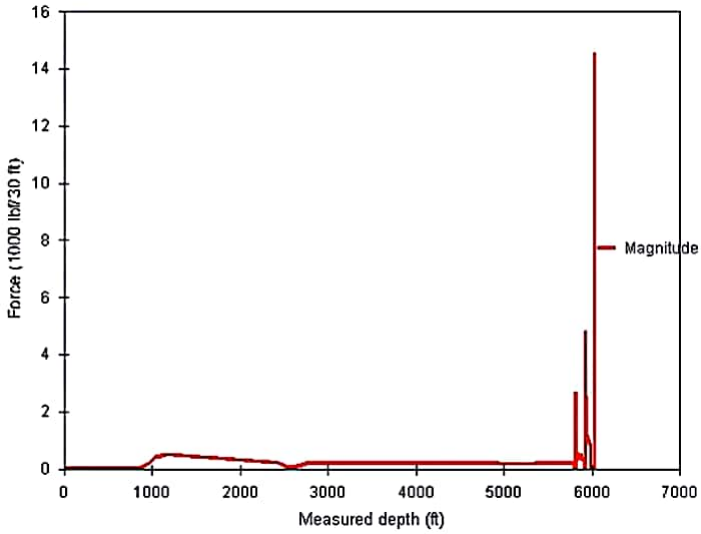

Fig. S2. Interaction of well and drill string in 16-inch hole.

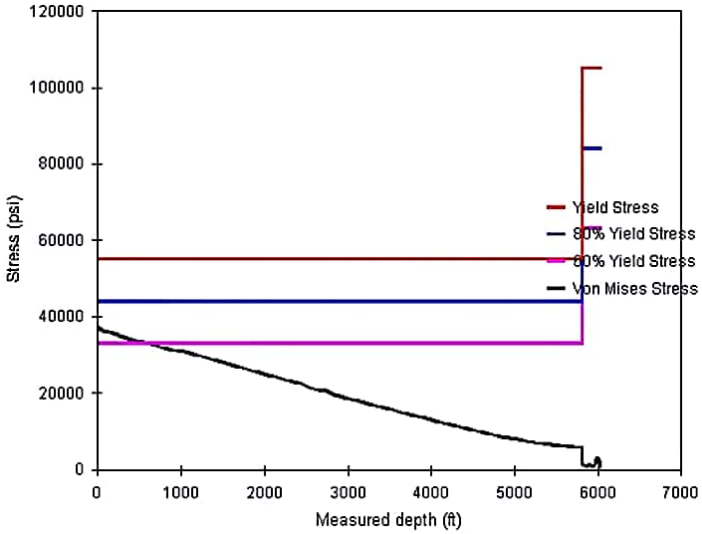

Fig. S3. Comparison of stresses and von Mises graph with measured depth in 16-inch hole.

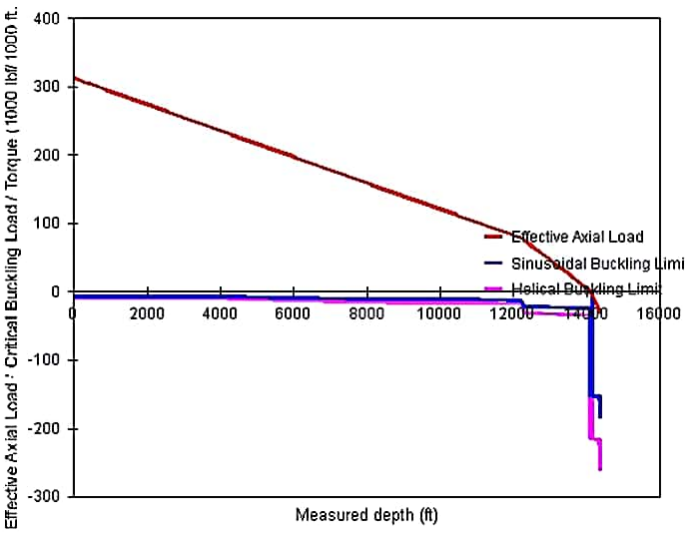

Fig. S4. Effective axial load in 12 ¼-inch hole.

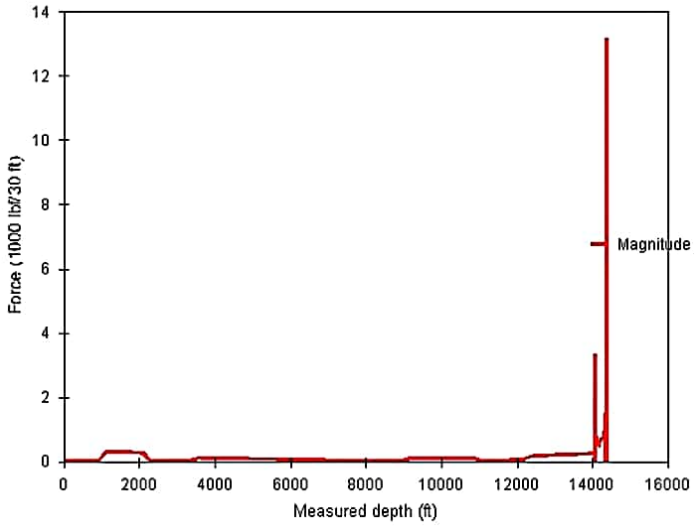

Fig. S5. Interaction of well and drill string in 12 ¼-inch hole.

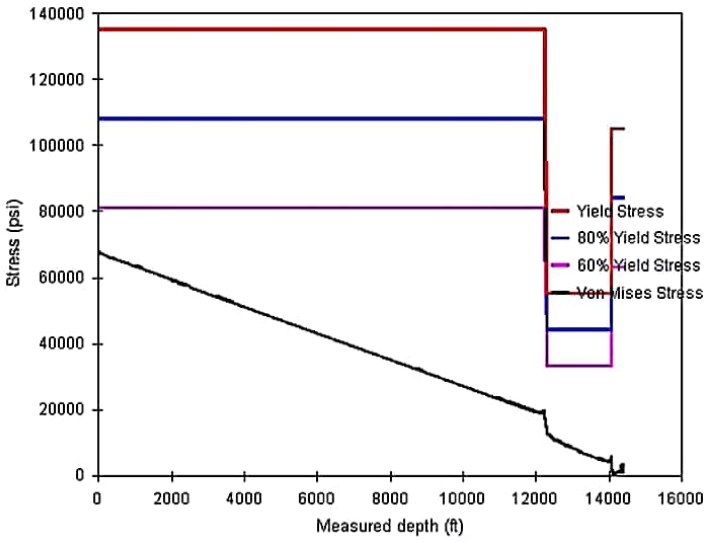

Fig. S6. Comparison of stresses and von Mises graph with measured depth in 12 ¼-inch hole.

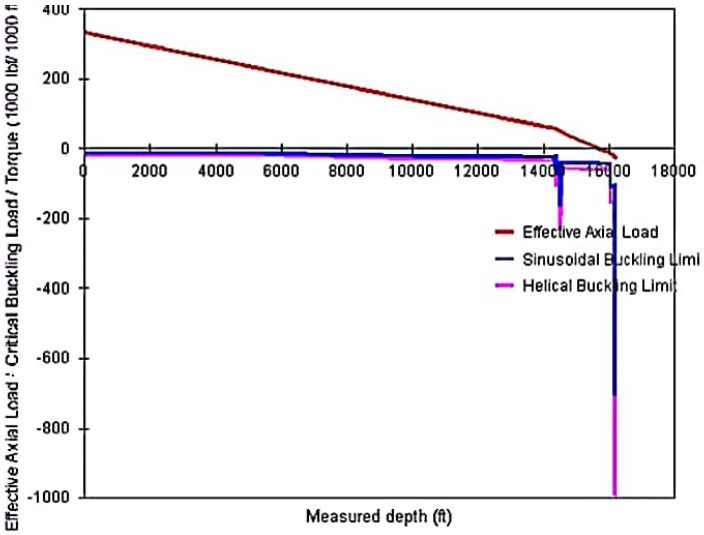

Fig. S7. Effective axial load 8 ½-inch hole.

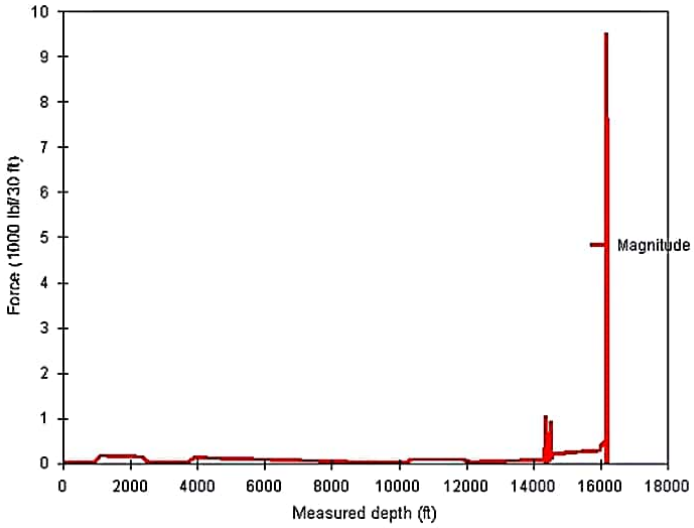

Fig. S8. Interaction of well and drill string in 8 ½-inch hole.

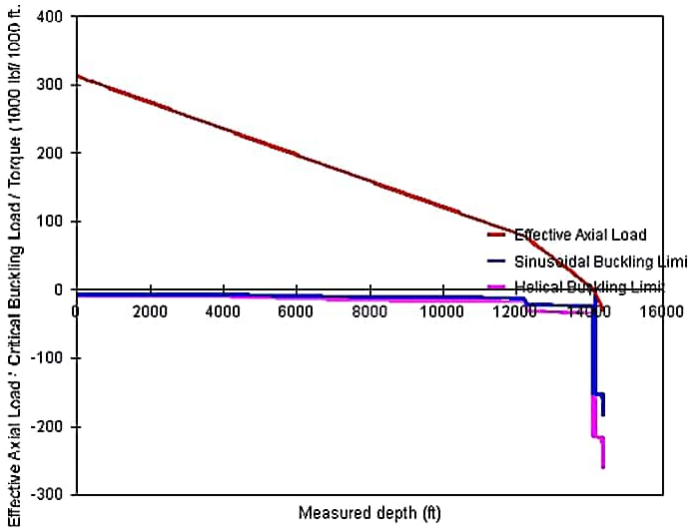

Fig. S9. Comparison of stresses and von Mises graph with measured depth in 8 ½-inch hole.

Hydraulics data:

Table S4. Hydraulic results in 16-inch hole.

	Volume (bbl)	Time (mins)	Strokes
Full circulation	1631.72	75.15	13266
Inside drill string	102.08	4.76	830
Annulus [bottoms up]	1529.64	71.38	12436
Bit to shoe	560.07	26.14	4553
Shoe to surface	969.57	45.25	7883

Table S5. Hydraulic results in 12 ¼-inch hole.

	Volume (bbl)	Time (mins)	Strokes
Full circulation	1995.57	111.75	16224
Inside drill string	248.55	13.92	2021
Annulus [bottoms up]	1747.02	97.83	14203
Bit to shoe	994.08	55.67	8082
Shoe to surface	752.94	42.16	6121

Table S6. Hydraulic results in 8 ½-inch hole.

	Volume (bbl)	Time (mins)	Strokes
Full circulation	1040.36	79.45	8458
Inside drill string	282.82	21.60	2299
Annulus [bottoms up]	757.55	57.85	6159
Bit to shoe	81.47	6.22	662
Shoe to surface	676.08	51.63	5497

.

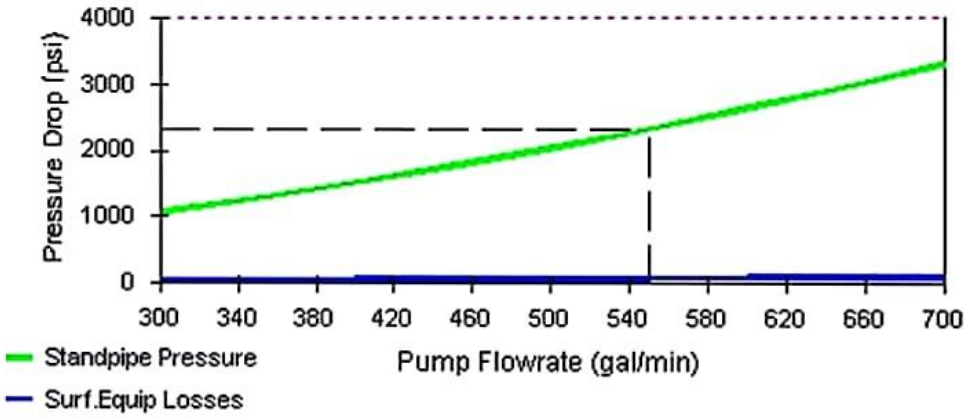

Fig. S14. The sensitivity of pressure drop to the pump flow rate in standpipe and surface equipment in 8 ½-inch hole.

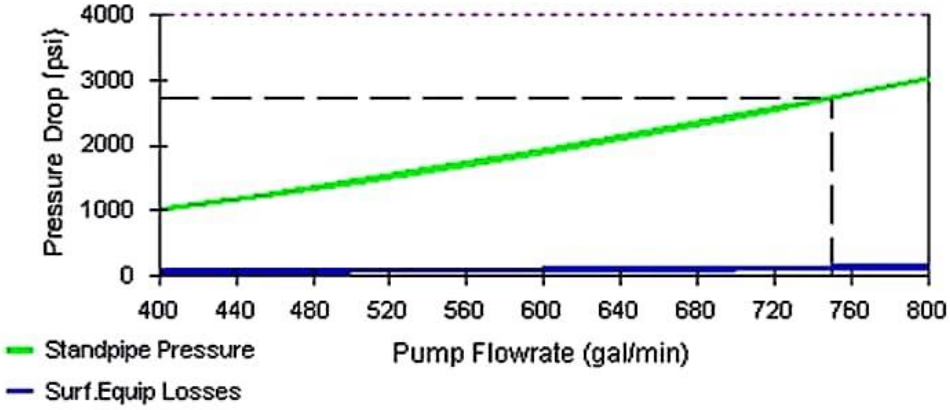

Fig. S12. The sensitivity of pressure drop to the pump flow rate in standpipe and surface equipment in 12 ¼-inch hole.

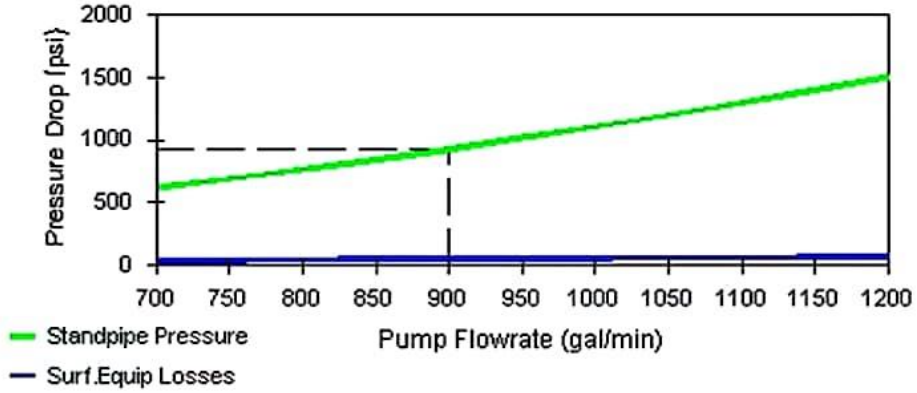

Fig. S10. The sensitivity of pressure drop to the pump flow rate in standpipe and surface equipment in 16-inch hole

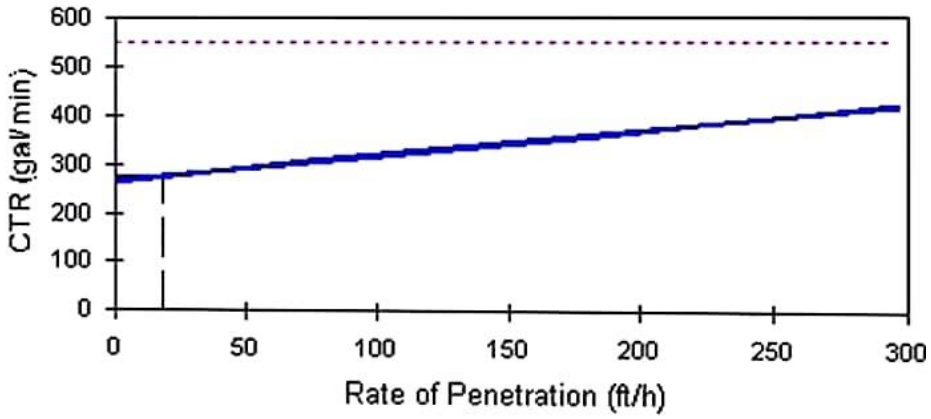

Fig. S15. Relationship between critical required rates to clean up annulus versus rate of penetration in 8 ½-inch hole.

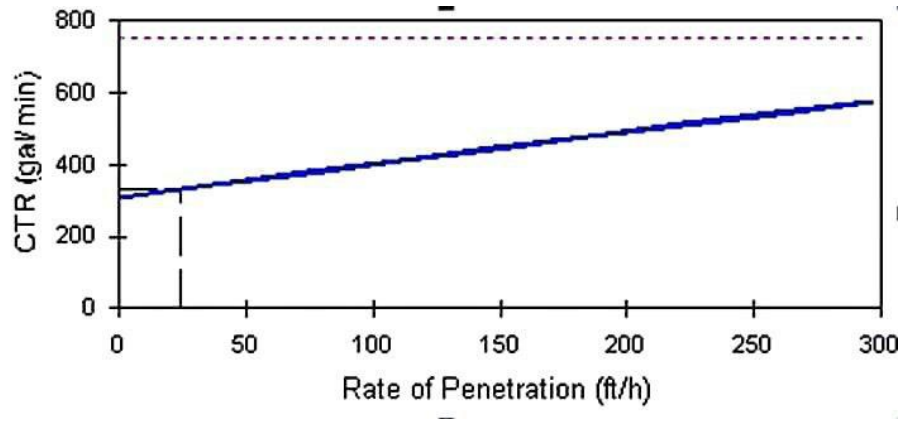

Fig. S13. Relationship between critical required rates to clean up annulus versus rate of penetration in 12 ¼-inch hole.

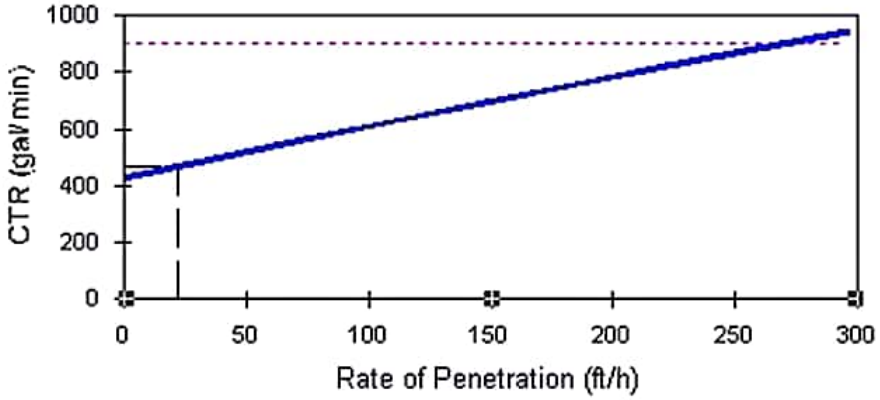

Fig. S11. Relationship between critical required rates to clean up annulus versus rate of penetration in 16-inch hole.